buildings

MDPI

Article

Case Study of Space Optimization Simulation of Existing Office Buildings Based on Thermal Buffer Effect

Shenqi Gan [1,2,*], Wenxiang Chen [1,2] and Jiawang Feng [1,2]

[1] School of Architecture and Planning, Anhui Jianzhu University, Hefei 230601, China; chenwx@stu.ahjzu.edu.cn (W.C.); fengjw@stu.ahjzu.edu.cn (J.F.)
[2] Key Laboratory of Built Environment and Health, Anhui Jianzhu University, Hefei 230601, China
* Correspondence: gansq@ahjzu.edu.cn

Abstract: This paper takes an old office building in Hefei as the research object to explore the influence of the thermal buffering performance of the case building buffer space on the air speed and thermal environment of the office space based on the field measurement and simulation. As the thermal buffer layer of the main space, the buffer space is the layout mode that follows the thermal transfer law. Building buffer space variables were evaluated and compared by orthogonal tests to determine the better combination of buffer space sizes. The results show that when the air speed is taken as the evaluation index, the influence of each buffer space on the indoor environment is ordered: courtyard > corridor > foyer; when the temperature is taken as the evaluation index, the influence of each buffer space on the indoor environment is ordered: courtyard > foyer > corridor. From the perspective of green transformation, this paper selects two better schemes. Through comparison, it is found that when the buffer space size is: corridor (16 m × 2 m × 3.3 m), courtyard (16 m × 12 m) and foyer (7.2 m × 6 m × 3.3 m) is the optimal scheme, the indoor air speed is increased by 0.1 m/s, and the temperature is reduced to 27.0 °C, which is within the thermal comfort range of the human body. It is found that optimizing the buffer space size of the case building can effectively improve its indoor air speed and thermal environment, and provide theoretical basis and reference for the green transformation of existing buildings of the same type in this area.

Keywords: existing buildings; thermal buffer effect; office space; buffer space; green; transformation; CFD simulation

check for updates

Citation: Gan, S.; Chen, W.; Feng, J. Case Study of Space Optimization Simulation of Existing Office Buildings Based on Thermal Buffer Effect. *Buildings* **2024**, *14*, 1611. https://doi.org/10.3390/buildings14061611

Academic Editor: Jiying Liu

Received: 22 April 2024
Revised: 26 May 2024
Accepted: 27 May 2024
Published: 1 June 2024

Copyright: © 2024 by the authors. Licensee MDPI, Basel, Switzerland. This article is an open access article distributed under the terms and conditions of the Creative Commons Attribution (CC BY) license (https://creativecommons.org/licenses/by/4.0/).

1. Introduction

According to the International Energy Agency (IEA) [1], about one-third of the world's energy consumption and CO_2 emissions are generated by the building sector, and the energy conservation and emission reduction of buildings is a common concern in urban renewal. On 11 March 2022, the Ministry of Housing and Urban-Rural Development issued the "14th Five-Year Plan for Building Energy Efficiency and Green Building Development", which requires that more than 350 million m^2 of energy saving renovation of existing buildings should be completed by 2025 [2]. At present, building renovation [3,4] mostly focuses on building function and form and lacks consideration of physical space and the thermal environment [5,6], and a large number of buildings have difficulty in meeting the national green and sustainable development requirements in terms of energy conservation and emission reduction, health, comfort, and economy, resulting in problems such as lack of livability and inefficient environmental performance [7,8]. In order to solve the problem between architecture and the environment, many architects at home and abroad have carried out a lot of practical explorations, such as the Dutch architect Herman, who proposed the theory of "intervening space", Aldo van Eyck established the theoretical system of "intermediary space" [9], and the Japanese architect Kisho Kurokawa proposed the concept of "gray space" [10,11]. Chinese architect Song proposed the concept of

"bioclimatic buffer layer" from the perspective of energy exchange between the outside and the interior of the building [12]. Li proposed the concept of the "Building cavities" based on architectural bionics, with the help of the building cavity to achieve the purpose of regulating the indoor thermal environment [13]. Deng analyzed the influence of building cavities on the indoor air speed environment through simulations [14]. Wang transformed the traditional ecological experience of Qinghai Zhuangkuoyuan at the spatial level and used the concept of the "architectural cavity" to integrate the ecological and functional needs of the building [15]. Chen investigated the difference between the inner and outer spatial levels affected by outdoor thermal in the natural state by measuring the winter and summer temperature of a campus building in Nanjing, and the results showed that the mode of the main space inside and the buffer space outside had a thermal buffering effect [16]. Zhao proposed a plane layout optimization strategy suitable for different climate zones based on the analysis of the relationship between the buffer thermal effect and the layout pattern of the auxiliary space based on the simulation data [17]. Through the comparison of research on the spatial thermal buffer at the domestic level and abroad, it can be found that foreign theoretical research is earlier, the application of the thermal buffer is relatively mature, and the method of combining performance with form is expanded and applied, such as the "tubular housing theory" and "open space theory" summarized by Indian architect Charles Correa. In contrast, domestic research started late, and the development is uneven, lacking understanding of regional climate characteristics and traditional forms.

At present, there are relatively few studies on the integration design of building energy saving technology and building space. Usually, the building space is organized before the energy saving design, and then additional energy saving optimization is conducted according to the thermal environment characteristics of the building space after the design [18]. In this paper, according to the climate characteristics of Hefei, Anhui Province, an old office building in the city is taken as an example; the temperature and air speed in the case building are measured by means of fixed monitoring point, and the relationship between the buffer space and the air speed and thermal environment of the main indoor space is studied. Based on theoretical research, actual measurement, and simulation analysis, the influence of the buffer space with the thermal buffer effect on the indoor thermal environment of the case building is summarized, and on this basis, the buffer space of the case building is optimized to meet the needs of the building, improve its indoor air speed and thermal environment, and provide reference for the green transformation of the same type of existing office buildings in the region.

2. Research Overview and Methodology

2.1. Research Framework

In this paper, the buffer space of case buildings is studied, and the methodology framework adopted includes field testing, optimization index selection, simulation, analysis, and discussion, as shown in Figure 1. In field tests, the information of the case building and the analysis of the measured data are studied, and the thermal buffer effect of the buffer space is expounded. Secondly, in the simulation, variance and range analyses are carried out through the results of single-variable and multivariate combined simulation, and the optimal combination of buffer space is summarized. Finally, through the comparison with the existing research, it is concluded that this study provides reference for the green transformation of the same type of buildings.

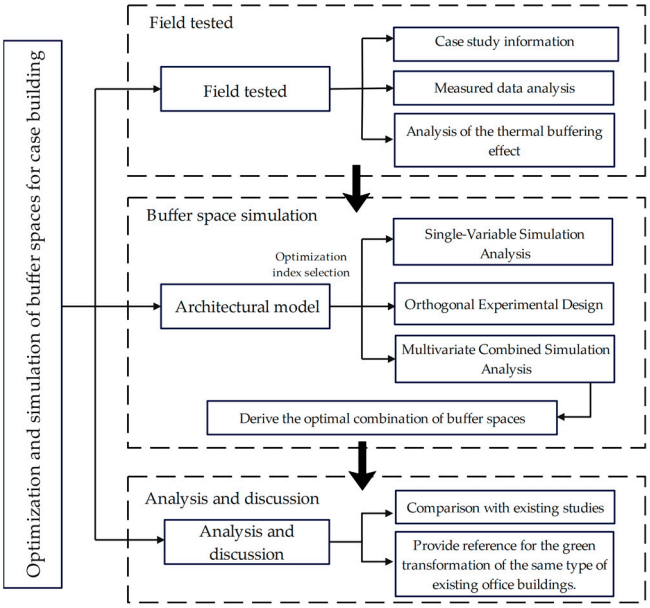


Figure 1. Overview of the research approach and workflow of this study.

2.2. Research Area and Object

Hefei is located in the middle latitude zone, 31°86′ N, 117°27′ E. It is one of the regions with the most obvious monsoon climate and a typical representative city with a hot summer and cold winter region. The annual temperature is cold in winter and hot in summer, mild in spring and autumn, which belongs to the warm-temperate to subtropical transition zone. The annual average temperature is between 15 and 16 °C, the average temperature in summer is about 27.5–28.5 °C, and the average temperature in winter is between 1.5 and 5.0 °C. The dominant wind direction of the city is southeast wind, with southeast wind in summer and northeast wind in winter, with an annual average air speed between 1.6 and 3.3 m/s.

This paper selects an old office building in Hefei City as the research object, which was built in the 1950s. The current situation is shown in Figure 2. The main body of the building is an imitation of the Soviet style, facing the south to the north. The building has three floors, with a construction area of 2910 m^2. The plane is "I" shaped with axial symmetry. The space organization form is the outer corridor ladder, the building is the brick structure, the facade is painted with green/gray paint, the doors and windows are wooden, sprayed with red paint, the roof is a Chinese sloping roof, and specific envelope structures are shown in Table 1.



Figure 2. Current status of the office building.

Table 1. Main envelope structure materials and performance parameters.

		Envelope Construction	Thermal Transfer Coefficient K/(W/(m^2·K))	Thermal Resistance of Thermal Conductivity R/[(m^2·K)/W]
Name of envelope structures	Outside the wall	5 mm green/gray paint 10 mm cement mortar plastering 240 mm clay brick 20 mm plaster mortar plastering	1.88	0.53
	Floor	10 mm terrazzo ceramic tile veneers 20 mm cement mortar plastering 120 mm concrete slab 20 mm cement mortar plastering	3.57	0.28
	Doors and windows	40 mm wooden door 6 mm single-layer clear glass	2.5 5.88	0.4 0.17

2.3. Measurement Method

In this paper, the air and thermal environmental test was conducted on the building space of the case, and the time selected was from 8:00 to 18:00 on 29 July 2023, with a total of 10 h of uninterrupted testing. Using fixed monitoring, automatically record data every ten minutes, test parameters including temperature and humidity and air speed. Arrange 7 measuring points, distributed in the first floor outdoor, north and south side office space, and buffer space including: entrance hall, corridor, stairs, toilet. By comparing the indoor and outdoor temperature levels, the red solid circles are the measuring points of air temperature and air speed. The specific measuring point layout is shown in Figure 3. According to the "Standard for Testing Methods for Building Thermal Environment" JGJ/T347-2014 [19], the test height is the main activity height of personnel, 1.1 m from the ground, as shown in Figure 4. The name, photo, function, model, measurement range, and measurement accuracy of the test instrument are shown in Table 2.

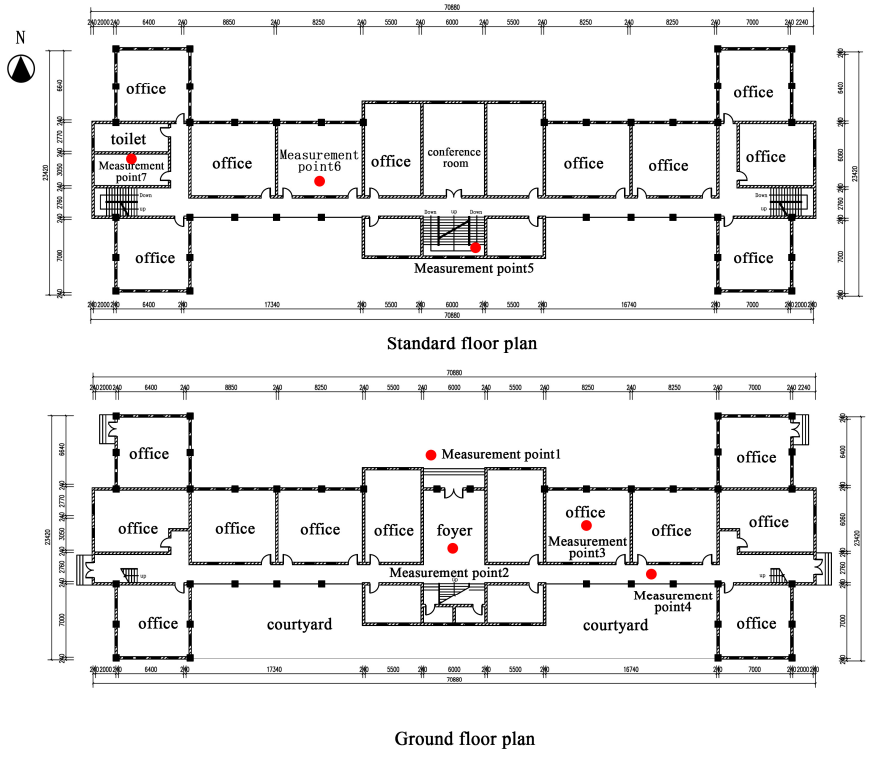


Figure 3. Schematic diagram of the plane measurement points of the office building.



Figure 4. Measured view of the office area. (The anemometer is 1.5 m from the ground, and the temperature and humidity instrument is 1.1 m from the ground).

Table 2. List of measurement instruments.

Instrument Name	Measurement Parameters	Measuring Range	Accuracy	Resolution	Instrument Picture
American Kestrel 5500 Handheld Anemometer	air velocity (m/s)	0.3~40 m/s	±3%	0.1 m/s	
Germany testo 174H humidity and temperature recorder	temperature (°C)	−20~70 °C	±0.5 °C	0.1 °C	
	humidity (RH)	0~100%RH	±3%RH	0.1%RH	

2.4. Analogy Method

In this paper, CFD Phoenics2019 software was used to simulate and compare qualitatively and quantitatively analyze the office building [20]. The model is built in Sketchup, and the Phoenics software is imported, boundary conditions and climate data are input, turbulence, temperature, and radiation equations of the model are opened, and the doors and windows were all open in the simulation process, so the simulation result diagram of indoor air speed and temperature is obtained through simulation calculation, and the results related to the evaluation index are extracted.

2.4.1. Boundary Condition Setting

The simulation site is set as Hefei, Anhui, China (31°86′ N, 117°27′ E), and the simulation time is selected as July 29 in summer. According to the measured data, the initial air speed in the study area is set as 0.5 m/s, the dominant wind direction is southeast wind,

the reference height is 10.0 m, and the ambient temperature is 29 °C. And the model size is 70.88 m (east–west direction), 23.42 m (north–south direction), 12.10 m (the height is the highest point of the building). The calculated height of the general simulated region is three times that of the original model, the calculated length and width are five times the nature of the original model, the model calculation domain is set to 350 m × 120 m × 40 m, and the model parameters are set as shown in Table 3.

Table 3. Model parameter settings.

Model Volume	Hx = 70.88 m, Hy = 23.42 m, Hz = 12.10 m
Compute domains	Area 350 m × 120 m × 40 m
Geographical orientation	31°86′ N, 117°27′ E
Background temperature	26~29 °C
Background humidity	87%RH
Background air speed	0.5 m/s
Reference height	10.0 m
Background pressure	100,400 Pa
Turbulence model	*k*-ε model standard model
Simulation iterations	1500

2.4.2. Grid Division and Convergence Calculation

Meshing significantly affected the simulation results. Intensive mesh division can improve accuracy., The main part should be denser, and the other parts can be sparse to reduce the computational burden. In this paper, a dense grid of 0.25 m × 0.25 m is used in the target model area, and the surrounding area is 0.5 m × 0.5 m. The total calculation area grid is about 15 million, the number of iterations is set to 1500, and each simulation calculation is about 6 h. In order to verify the influence of grid settings on simulation results, two control schemes were set: 1 m × 1 m grid in the target area, 2 m × 2 m grid in the surrounding area, 0.5 m × 0.5 m grid in the target area, and 1 m × 1 m grid in the surrounding area, as shown in Table 4. Each scheme was simulated and the air speed was used as the index for evaluation and comparison. It was found that the probe value results of the three different grids were 0.0242 m/s, 0.0225 m/s, and 0.0253 m/s, and the average air speeds of the whole region were 0.281 m/s, 0.315 m/s, and 0.306 m/s. As shown in Figure 5, it can be found that the grid change is relatively insensitive to the change in air speed, indicating that the simulation is robust. In order to improve the accuracy and speed of calculation, a dense grid of 0.25 m × 0.25 m was selected for the target model area, and the surrounding area was 0.5 m × 0.5 m, as shown in Figure 6.

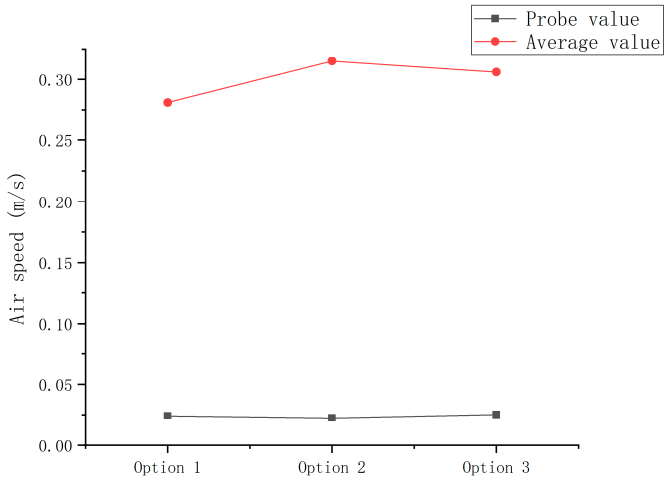
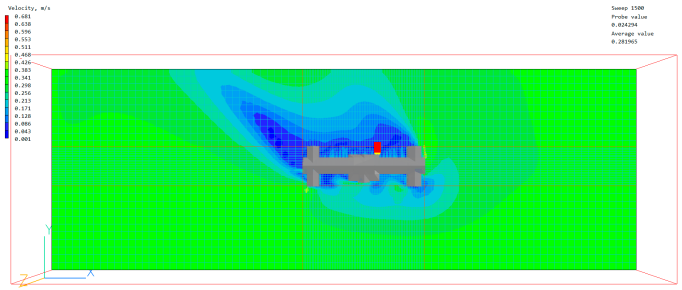
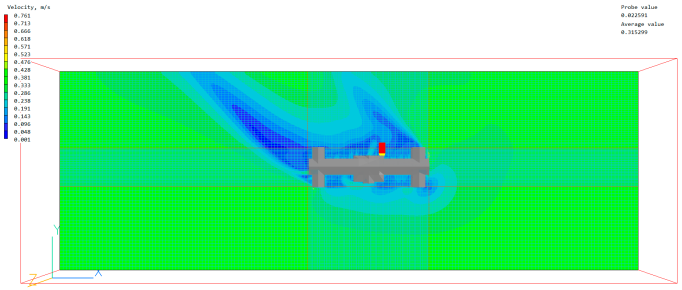
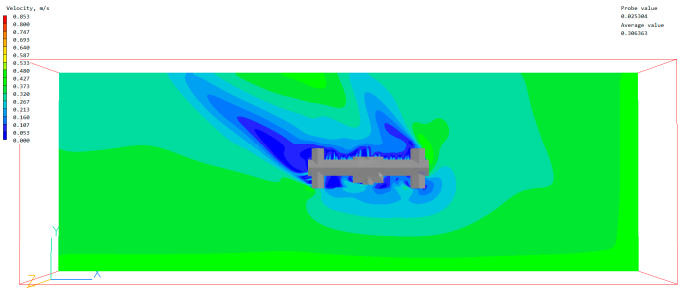


Figure 5. Simulation results of different grid divisions.

Table 4. Simulation verification of different grid divisions.

	Target Area Mesh Size	Surrounding Area Mesh Size	Total Grid Number	Simulation Result Cloud Image
Option 1	1 m × 1 m	2 m × 2 m	About 0.45 million	
Option 2	0.5 m × 0.5 m	1 m × 1 m	About 1.7 million	
Option 3	0.25 m × 0.25 m	0.5 m × 0.5 m	About 15 million	

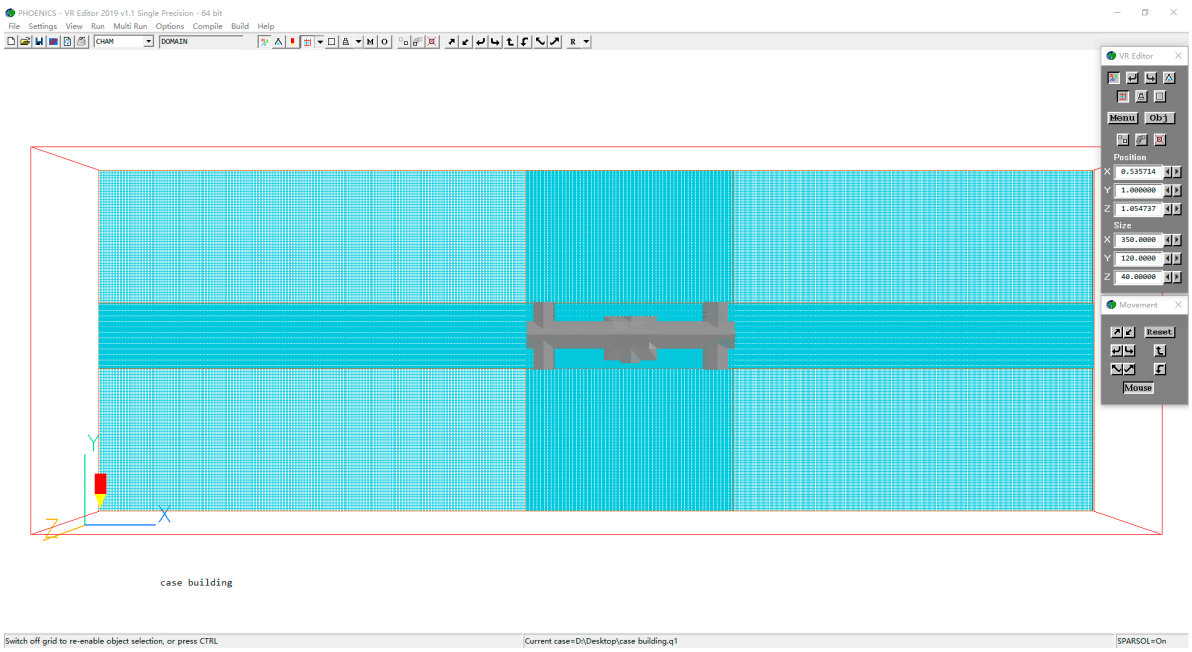


Figure 6. Phoenics software grid division.

In the Phoenics software setting, the initial wind field is set as the gradient wind field; the *k*-*ε* model has small fluctuation and high accuracy in numerical calculation, which is widely used in low-speed eddy flow and is easy for grid adaptation. The standard equation for *k*-*ε* is as follows [21]:

$$\begin{cases} \frac{\partial}{\partial t}(\rho k) + \frac{\partial}{\partial x_i}(\rho k u_i) = \frac{\partial}{\partial x_j}\left[\left(\mu + \frac{\mu_t}{\sigma_k}\right)\frac{\partial k}{\partial x_j}\right] + G_k + G_b - \rho\varepsilon - Y_M + S_k \\ \frac{\partial}{\partial t}(\rho \varepsilon) + \frac{\partial}{\partial x_i}(\rho \varepsilon u_i) = \frac{\partial}{\partial x_j}\left[\left(\mu + \frac{\mu_t}{\sigma_\varepsilon}\right)\frac{\partial \varepsilon}{\partial x_j}\right] + C_{1\varepsilon}\frac{\varepsilon}{k}\left(G_k + C_{3\varepsilon}G_b\right) - C_{2\varepsilon}\rho\frac{\varepsilon^2}{k} + S_\varepsilon \end{cases}$$

In the formula:
k—Turbulent kinetic energy;
ε—Dissipation rating;
μ—Hydrodynamic viscosity;
μ_t—Turbulence viscosity;
μ_i—Time averaged velocity;
ρ—Fluid density;
t—Time;
G_k—Turbulent kinetic energy generated by the laminar velocity gradient;
G_b—Turbulent kinetic energy generated by the buoyancy force;
Y_M—Fluctuations arising from the diffusion of the transitions in compressible turbulence;
$C_{1\varepsilon}$, $C_{2\varepsilon}$, $C_{3\varepsilon}$—Constant;
σ_k and σ_ε—Turbulent Prandtl numbers for equations k and ε;
S_k and S_ε—User-defined parameters.

2.5. Data Processing and Evaluation

2.5.1. Data Processing

For the data processing of field monitoring, exclude invalid data and outliers, average the hourly data, and make corresponding charts for preliminary analysis to determine the indicators and factors of buffer space optimization simulation. IBM SPSS Statistics 26 software was used to design an orthogonal experimental setup to determine the combination scheme of the simulation. Variance and range analyses were performed on the simulation results for the significance p of different index factors, where p value represents the significance level. When $p \leq 0.05$, it indicates a 95% confidence interval, so as to judge the optimal combination of indexes for the impact of buffer space on indoor environment.

2.5.2. Evaluating Indicator

According to the "Office Building Design Standard" JGJ/T67-2019 [22], for Class I and II office buildings, the indoor temperature in summer shall be 24 °C~26 °C, and the indoor air speed shall be 0.25 m/s. For Class III office buildings, the recommended indoor temperature in summer is between 26 °C and 28 °C, with an indoor air speed of less than or equal to 0.3 m/s. According to the "Hefei Energy Saving Design Standard for Public Buildings" DB34/T 5060-2016 [23], the indoor temperature of office buildings in summer should be between 26 °C and 27 °C. Therefore, the indoor air temperature of the case building should be between 26 °C and approximately 28 °C, and the indoor air speed range should be between 0.05 m/s and approximately 0.3 m/s.

3. Test Results and Analysis

3.1. Test Results

3.1.1. Indoor Temperature

After calculating the average temperature during the case building test, the hourly pattern can be obtained, as shown in Figure 7 and Table 5. According to the chart, during the test period, the outdoor temperature fluctuated between 26.9 and 29.3 °C, the peak appeared around 13:00, and the trough appeared around 18:00. The temperature fluctuation of the buffer space is between 26.3 and 28.81 °C, the peak appears at about 13:00 of the measuring point of the hall, and the trough appears at about 18:00. The temperature

fluctuation of the main office space is between 26.4 and 29.1 °C, the peak appears at about 13:00 of the measurement point of the standard office, and the trough appears at about 18:00 of the measurement point of the standard office. Due to the noon shower during the test period, the temperature fluctuation occurred between 12:00 and 14:00, and the temperature of each test point generally showed a "rise-down" trend.

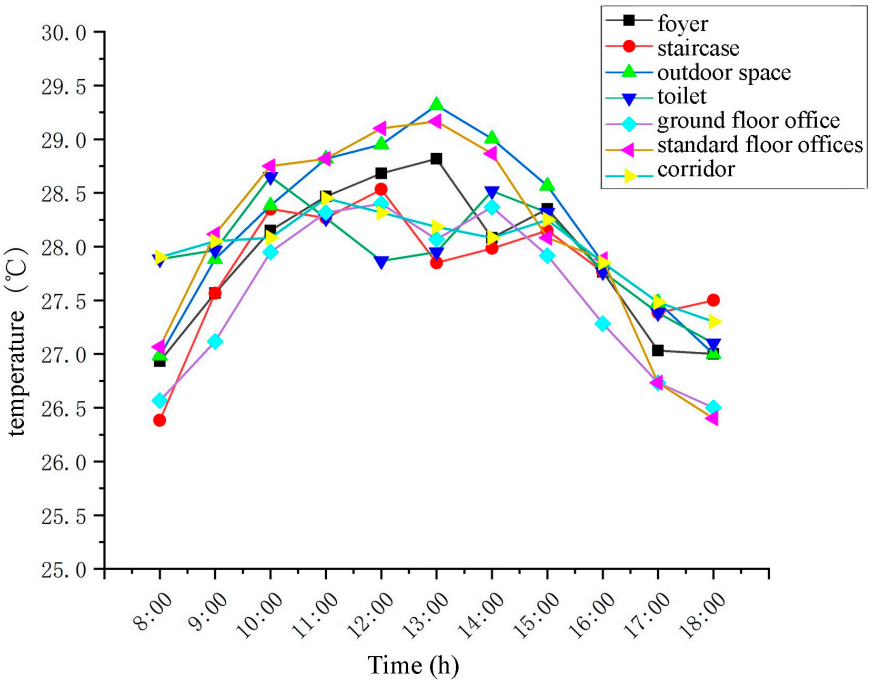


Figure 7. Comparison of indoor and outdoor temperatures.

Table 5. Overview of the temperature of each measuring point in the office building.

		Maximum (°C)	Minimum (°C)	Average Value (°C)	Standard Deviation	Range
Outdoor space	Outdoor on the first floor	29.30	26.90	28.20	1.69	2.40
Buffer space	Foyer	28.81	26.90	27.90	1.35	1.91
	Staircase	28.53	26.30	27.79	1.57	2.23
	Toilet	28.65	27.10	27.97	1.09	1.55
	Corridor	28.45	27.30	28.00	0.81	1.15
Indoor office space	Ground floor office	28.40	26.50	27.57	1.34	1.90
	Standard floor offices	29.50	26.40	28.09	1.90	2.70

3.1.2. Indoor Air Speed

After calculating the average air speed during the case building test, the hourly pattern can be obtained, as shown in Figure 8 and Table 6. It can be seen from the chart that in the air speed variation law, the time and size of the extreme value are different in different spaces. It can be seen that the fluctuation range of outdoor air speed is relatively large, 0.13~0.74 m/s, the peak is around 10:00, and the trough is around 15:00. The air speed fluctuation range in the buffer space is between the range of 0~0.34 m/s, and the peaks are around 9:00 and 13:00. During the test period, the doors and windows of the indoor

office space are closed, resulting in the indoor air speed basically being 0 m/s, and the air mobility is poor.

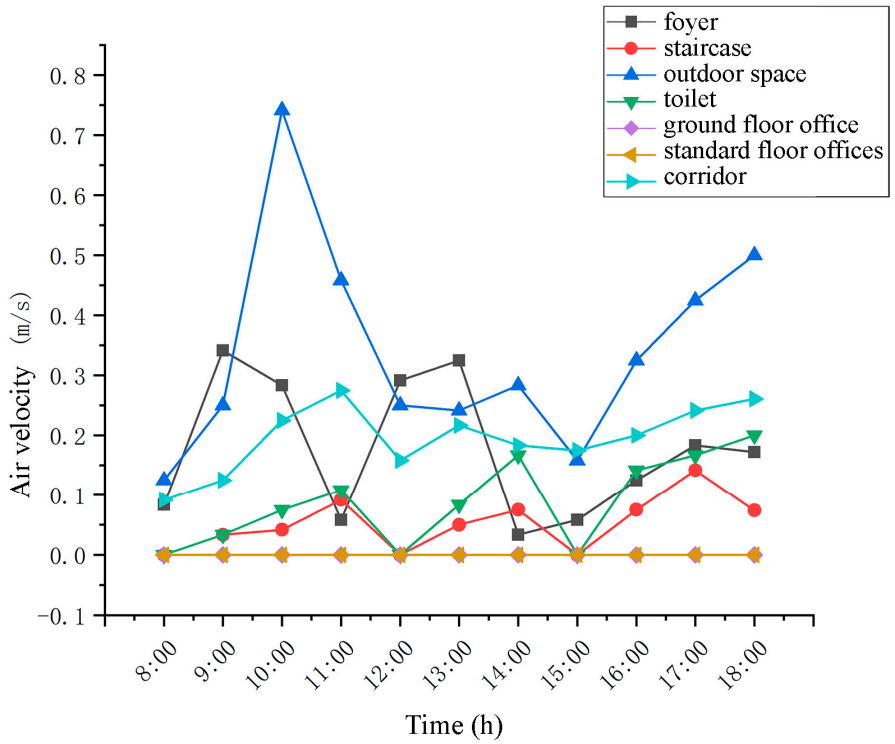


Figure 8. Comparison of the indoor and outdoor air speeds.

Table 6. Overview of air speed at each measurement point in the office building.

		Maximum (m/s)	Minimum (m/s)	Average Value (m/s)	Standard Deviation	Range
Outdoor space	Outdoor on the first floor	0.74	0.13	0.33	0.43	0.61
Buffer space	Foyer	0.34	0.03	0.18	0.21	0.31
	Staircase	0.14	0	0.05	0.09	0.14
	Toilet	0.17	0	0.08	0.12	0.17
	Corridor	0.28	0.09	0.19	0.13	0.19
Indoor office space	Ground floor office	0	0	0	0	0
	Standard floor offices	0	0	0	0	0

3.2. Analysis of the Test Results

Through the comparative analysis of the test results, the following conclusions were obtained:

(1) Through the measured data of different buffer spaces, it can be found that the outer corridor buffer space, courtyard buffer space, and staircase buffer space on the south side can produce better shading effect, reduce the solar radiation thermal in the internal space, and form a certain temperature gradient between the interior and the exterior. It is verified that the outer corridor, stairs, and courtyard on the south side have the thermal buffer potential and can play the role of climate buffer.

(2) The temperature of the indoor space < the temperature of the buffer space < the temperature of the outdoor space, indicating that the transitional buffer space can improve the indoor temperature [24], but it can be found that the temperature difference between the indoor and outdoor spaces during the measured period is small, which also indicates that the buffer space in the building has a weak ability to regulate the indoor temperature.

(3) The air speed of indoor < air speed of buffer space < air speed of outdoor, indicating that the buffer space can improve indoor air speed, and it can be found that its ability to regulate indoor air speed is weak. Proper buffer space design can effectively promote natural ventilation and remove excess thermal buffer, thus creating a healthy and comfortable building environment.

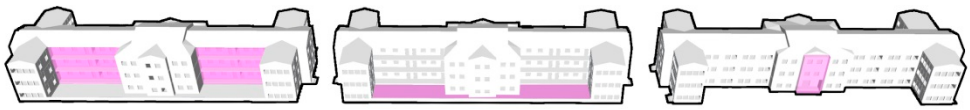
Through the analysis of temperature and air speed in different spaces, it is shown that there are certain differences in the performance of the air speed and thermal environment of the indoor and outdoor spaces of the building in the natural state. The buffer space is affected by the outdoor air speed and thermal environment. Through the transmission and adjustment of energy, the air and thermal environment of the indoor space in the building system can reach a dynamic balance state, and the reasonable transformation and optimization can effectively reduce the building energy consumption and improve indoor health and comfort [25,26].

4. Buffer Space Optimization Simulation

4.1. Indicator Selection and Variable Settings

Through the actual measurement of the air speed and thermal environment of the case building, it is evident that there are big problems in the air speed and thermal environment of the office space of the building, and after field investigation and data analysis, it is known that the buffer space of the building can slow down the change in indoor space environment caused by the change in outdoor air speed and thermal environment [27–29]. Therefore, in the optimization process, the buffer space can be used to improve the indoor air speed and thermal environment and improve human health and comfort [30–32]. Therefore, this paper puts forward a targeted optimization scheme, mainly changing the buffer space [33], controlling the parameters of the indoor space, the standard office space (8.2 × 6 × 3.3 m), and using the multivariate combination method to simulate and analyze, in order to find the optimal buffer space combination. Finally, three factors are selected: corridor buffer space (A), the corridor, A1~A3; courtyard buffer space (B), the courtyard, B1~B3; foyer buffer space (C), the foyer, C1~C3, and the value of each factor is as shown in Table 7.

Table 7. The value of each influencing factor and spatial diagram.

Corridor Buffer Space		**Courtyard Buffer Space**		**Foyer Buffer Space**	
Corridor (A)	Size (Unit: m) 16 × 2 × 3.3 (A1) 16 × 2.5 × 3.6 (A2) 16 × 3 × 3.9 (A3)	Courtyard (B)	Size (Unit: m) 16 × 8 (B1) 16 × 10 (B2) 16 × 12 (B3)	Foyer (C)	Size (Unit: m) 7.2 × 6 × 3.3 (C1) 7.2 × 8 × 3.6 (C2) 7.2 × 10 × 3.9 (C3)
Spatial diagram					

4.2. Simulation and Analysis of the Original Model

Firstly, the simulation verifies the error value of the measured and the simulated data to ensure the accuracy of the simulation; secondly, the simulation shows the effects of different buffer spaces on the indoor air speed and thermal environment; finally, the best buffer space combination is found through the combination of multiple variables. Build up the original model of the measured office building, as shown in Figure 9. In order to speed up the computer convergence speed, the model is simplified; the modeling content includes

the internal and external walls of the building, column network, ground, floor, roof, and open the door holes and window holes on the wall. The simulation of the original model was performed according to the software setup and simulation requirements described above. After the simulation is completed, multiple points are selected for each buffer space and the average value is calculated to represent the average value of each space, as shown in Figure 10. The simulation results are shown in Figure 11. The measured values are strongly correlated with the simulated values, indicating that the parameter setting of the software is reasonable.

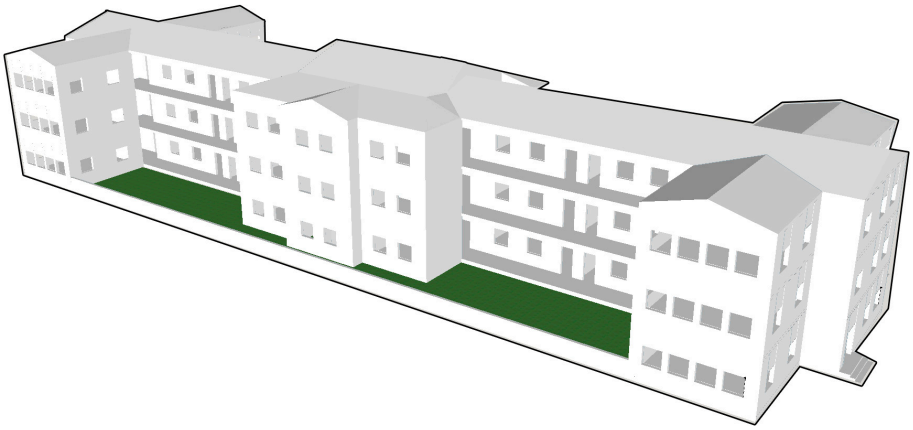


Figure 9. Case building of the original model.

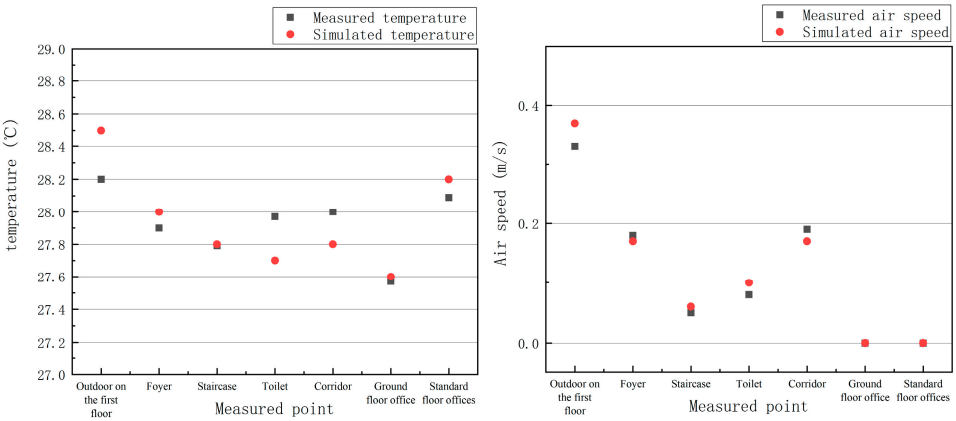
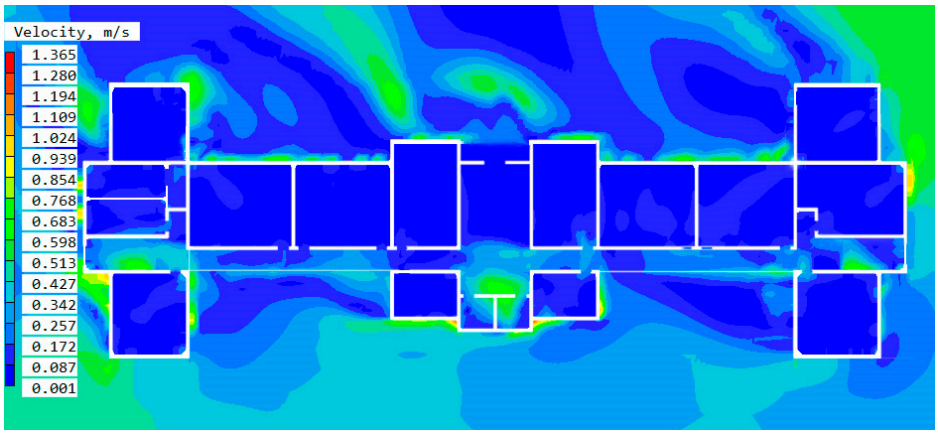
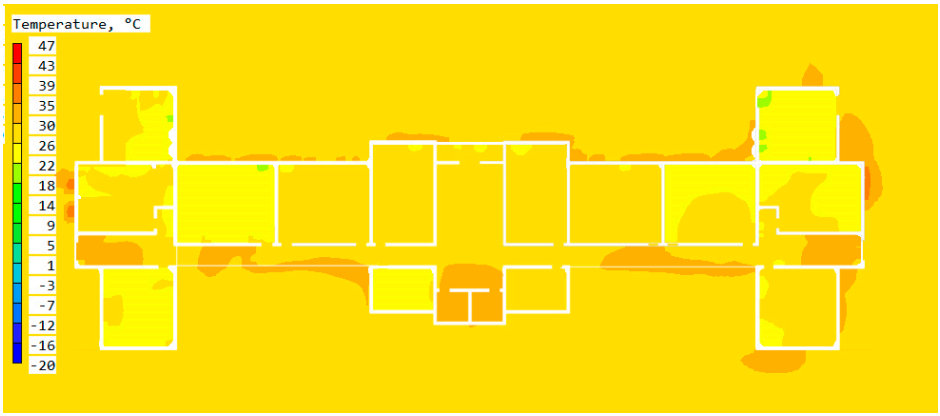


Figure 10. The measured value is compared with the simulated value.



(**a**)

Figure 11. *Cont.*



(**b**)

Figure 11. Simulation results of the original model: (**a**) air speed simulation results; (**b**) temperature simulation results.

4.3. Single-Variable Simulation Analysis

The calculation model and parameters were input into the Phoenics software, and the degree and trend of the air speed and temperature change in the office space under the single variable of the above three buffer spaces were studied. By comparing A0 (the original model without changing the buffer space, as shown in Figure 2), the indoor air speed of the indoor space rises to a maximum of 0.09 m/s under the factor value of B1, and the indoor temperature drops to a minimum of 27.1 °C under the factor values of A1, A2, and B1, as shown in Figures 12 and 13, respectively. The improvement in the indoor environment was not obvious for the remaining single variables.

The influence of the categorical and ordinal variables (factors) on the numerical variables (observed variables) was studied using an ANOVA to determine whether there is a relationship between them and the strength of the relationship. The basic principle is to decompose the changes in all observations by starting from the variance in the observed variables and to compare the systematic and random errors of the observed variables caused by the factors, thus inferring whether there are significant differences between samples [34]. The single-variable ANOVA investigates whether a control variable has a significant effect on the observed variable. If the p value is less than the α of the significance level, it is considered that there is a significant difference in the overall mean value of the observed variables at the level of the control variables. On the other hand, the control variables were considered to have no significant effect on the observed variables.

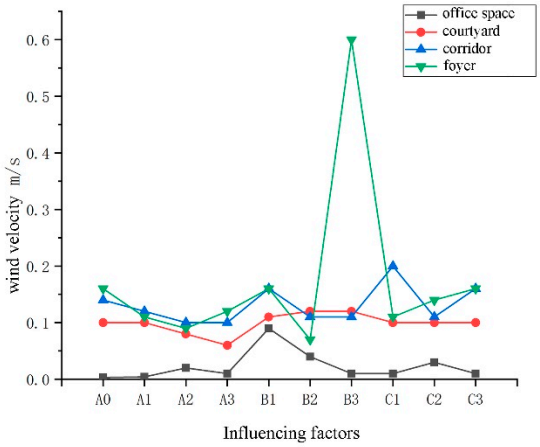


Figure 12. Single-variable air speed simulation results.

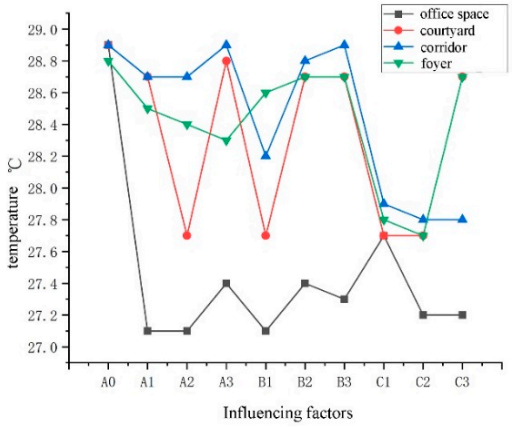


Figure 13. Single-variable temperature simulation results.

When the significance level was $\alpha = 0.05$, according to Table 8, the significance p value of each factor was greater than 0.05, indicating that there was no significant relationship between the three single factors of the corridor, courtyard, and foyer and the indoor air speed environment. According to Table 9, the significance p value of the corridor and foyer was greater than 0.05, and only the significance p value of the courtyard was less than 0.05, indicating that the two single factors of the corridor and foyer had no significant relationship with indoor temperature, and only the courtyard had a significant relationship with temperature. It can be seen that the change in a single factor cannot effectively improve the indoor air speed and thermal environment. Therefore, we need to further find the optimal combination through multivariate combination simulation analysis.

Table 8. Calculation results of the variance analysis of the indoor mean air speed simulated by single variable.

Influencing Factors	Sum of Squares	Degree of Freedom	Mean Square	Test Statistic F	Significance p
Corridor	0.001	2	0.000	0.245	0.720
Courtyard	0.005	2	0.002	2.213	0.171
Foyer	0.003	2	0.001	1.118	0.431

Table 9. Calculation results of ANOVA for the indoor mean temperature simulated by single variable.

Influencing Factors	Sum of Squares	Degree of Freedom	Mean Square	Test Statistic F	Significance p
Corridor	0.169	2	0.084	0.203	0.822
Courtyard	1.849	2	0.924	6.820	0.029
Foyer	0.629	2	0.314	0.928	0.447

4.4. Multivariate Combined Simulation Analysis

4.4.1. Orthogonal Experimental Design

From the above analysis, it can be seen that the change in a single factor to the indoor environment is not obvious, and thus, it is necessary to comprehensively analyze each factor. Orthogonal testing is a method of reducing the number of trials compared with comprehensive experiments, and it is an efficient method of experimental design by selecting representative samples from the comprehensive test portfolio according to certain rules [35]. Based on the sensitivity of each single factor and its relationship with the indoor air speed and thermal environment, the L_9 (3^4) orthogonal table was obtained using the SPSS26 software when studying the coupling effect of multiple factors, and the three-factor three-level orthogonal experiment method was used to reduce the number of multi-factor

experiments with the minimum influence, as shown in Table 10. Phoenics was used to simulate each group of experiments to study the influence of the interaction of various factor levels on the indoor air speed and thermal environment and predict the optimal combination of the whole experiment.

Table 10. Multi-factor orthogonal combination methods and results of indoor air–thermal environmental improvement.

Number	How the Buffer Space Is Combined	Average Indoor Air Speed (m/s)	Average Indoor Temperature (°C)
1	A3B3C1	0.05	28.5
2	A1B2C3	0.1	27.6
3	A3B1C3	0.01	27.1
4	A1B3C2	0.02	28.3
5	A2B3C3	0.01	28.3
6	A3B2C2	0.12	27.1
7	A2B2C1	0.02	28.0
8	A2B1C1	0.01	27.0
9	A1B1C1	0.02	27.8

4.4.2. Significance Analysis of the Influencing Factors

1. Range Analysis

The magnitude of the range value in the range analysis method reflects the influence of each factor on the experimental results, and the greater the range, the greater the impact on the experimental results, and vice versa [36]. Range analysis can determine the primary and secondary relationships between each factor in the indoor environment, and it can determine the optimal combination through the results of range analysis. Taking the indoor air speed as the evaluation index, it was concluded that the influence of each buffer space on the air speed of the indoor space was as follows: courtyard > corridor > foyer. The optimal levels are corridor (A3), courtyard (B2), and foyer (C2), as shown in Table 11. When the temperature was used as the evaluation index, the results of the influence of each buffer space on the temperature of the indoor space were obtained as follows: courtyard > corridor > foyer. The optimal levels are corridor (A1), courtyard (B3), and foyer (C1), as shown in Table 12.

Table 11. Analysis results of the multi-factor combination simulation air speed range.

Item	Level	Corridor (A)	Courtyard (B)	Foyer (C)
K avg	1	0.04	0.01	0.02
	2	0.01	0.08	0.07
	3	0.06	0.02	0.04
Optimal level		3	2	2
Range		0.05	0.07	0.04
Sort of factors			B > A > C	

Table 12. Simulated average temperature range analysis results of the multi-factor combination.

Item	Level	Corridor (A)	Courtyard (B)	Foyer (C)
K avg	1	27.9	27.3	27.82
	2	27.77	27.57	27.7
	3	27.57	28.37	27.67
Optimal level		1	3	1
Range		0.33	1.07	0.16
Sort of factors			B > A > C	

2. Multivariate analysis of variance

Because the range analysis cannot distinguish whether the experimental error corresponding to each level between the factors is caused by different factors or the experimental error, it cannot estimate the magnitude of the error and provide more accurate results. Therefore, multivariate analysis of variance was performed using the SPSS software, which investigates whether two or more control variables have a significant effect on the observed variables [34]. According to Table 13, when the significance level $\alpha = 0.05$, the significance of the indoor air speed was in the following order: courtyard > corridor > foyer. According to Table 14, the significant effects on the indoor temperature are courtyard > foyer > corridor, where the significance p value of the courtyard and foyer were 0.008 and 0.024, respectively, both of which were smaller than the significance level. The results showed that the courtyard and foyer had a significant effect on the indoor temperature, while the significance p value of the corridor was greater than 0.05, indicating that it had no significant effect on the indoor temperature.

Table 13. Calculation results of the variance analysis for multi-factor combination simulation of the indoor average air speed.

Influencing Factors	Sum of Squares	Degree of Freedom	Mean Square	Test Statistic F	Significance p
Corridor	0.003	2	0.002	1.405	0.416
Courtyard	0.007	2	0.004	3.027	0.248
Foyer	0.001	2	0.002	0.243	0.804

Table 14. Calculation results of the variance analysis for multi-factor combination simulation of the indoor average temperature.

Influencing Factors	Sum of Squares	Degree of Freedom	Mean Square	Test Statistic F	Significance p
Corridor	0.169	2	0.084	10.857	0.084
Courtyard	1.849	2	0.924	118.857	0.008
Foyer	0.629	2	0.314	40.429	0.024

When air speed was used as the evaluation index, the results of the range analysis and variance analysis were consistent, but the significance p value in the variance analysis was greater than the significance level. This indicates that when improving the buffer space, because the spatial shape tends to be flat, there is not enough height difference, which is not conducive to the use of hot pressure ventilation, and thus the indoor ventilation volume is easily affected by the season, wind direction, and air speed, resulting in unstable ventilation [37]. Since the influence of each factor on the results is not significant, there is no need to make multiple comparisons between the levels of each factor, and the optimal combination is A3B2C2 based on the results of the range analysis. When temperature was used as the evaluation index, the results of the range and variance were inconsistent; however, in the variance analysis, the significance p values of the courtyard and foyer were less than the significance level, while the significance p value of the corridor was greater than the significance level. The results were compared between the factor levels to determine the optimal level of the three factors, which were as follows: corridor, courtyard, and foyer, as shown in Tables 14–16.

Table 15. Multiple comparisons between different levels of the corridor.

Dependent Variable: Room Temperature LSD		Mean Difference (I − J)			95% Confidence Interval	
(I) Corridor	(J) Corridor		Standard Error	Significance	Lower Limit	Upper Limit
16 × 2 × 3.3	16 × 2.5 × 3.6	0.133	0.0720	0.205	−0.176	0.443
	16 × 3 × 3.9	0.333 *	0.0720	0.044	0.024	0.643
16 × 2.5 × 3.6	16 × 2 × 3.3	−0.133	0.0720	0.205	−0.443	0.176
	16 × 3 × 3.9	0.200	0.0720	0.109	−0.110	0.510
16 × 3 × 3.9	16 × 2 × 3.3	−0.333 *	0.0720	0.044	−0.643	−0.024
	16 × 2.5 × 3.6	−0.200	0.0720	0.109	−0.510	0.110

Based on average measured values. The error term is mean square (error) = 0.000. *, The significance level of the mean difference is 0.05.

Table 16. Multiple comparisons between different levels of the courtyard.

Dependent Variable: Room Temperature LSD		Mean Difference (I − J)			95% Confidence Interval	
(I) Courtyard	(J) Courtyard		Standard Error	Significance	Lower Limit	Upper Limit
16 × 8	16 × 10	−0.267	0.0720	0.066	−0.576	0.043
	16 × 12	−1.067 *	0.0720	0.005	−1.376	−0.757
16 × 10	16 × 8	0.267	0.0720	0.066	−0.043	0.576
	16 × 12	−0.800 *	0.0720	0.008	−1.110	−0.490
16 × 12	16 × 8	1.067 *	0.0720	0.005	0.757	1.376
	16 × 10	0.800 *	0.0720	0.490	0.490	1.110

Based on average measured values. The error term is mean square (error) = 0.000. *, The significance level of the mean difference is 0.05.

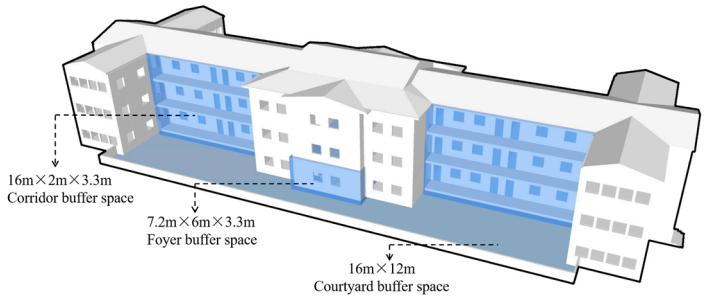
As can be seen from Table 15, the significance of A1 (16 m × 2 m × 3.3 m) and A3 (16 m × 3 m × 3.9 m) was 0.044, indicating that there is a significant correlation between the two, and because the mean difference between them is positive, the significance of A1 is higher than that of A3. As can be seen from Table 16, the significance of B1 (16 m × 8 m) and B3 (16 m × 12 m) was 0.005, and the mean difference between them was negative, indicating that the significance of B3 is higher than that of B1. The significance of B2 (16 m × 10 m) and B3 (16 m × 12 m) was 0.008, indicating that there is a significant correlation between them, and the mean difference between them was negative, indicating that the significance of B3 was higher than that of B2. As can be seen from Table 17, the significance of C1 (7.2 m × 6 m × 3.3 m) and C2 (7.2 m × 8 m × 3.6 m) was 0.013, and the significance of C1 (7.2 m × 6 m × 3.3 m) and C3 (7.2 m × 10 m × 3.9 m) was 0.027, indicating that there is a significant correlation between C1, C2, and C3, and because the mean difference between them was positive, the significance of C1 is higher than that of C2 and C3. Based on the multiple comparisons between the levels of various factors, the optimal combination was A1B3C1.

When the buffer space combination was A3B2C2, the simulation optimization results showed that the indoor air speed increased by 0.12 m/s, and the indoor temperature was 27.1 °C. When the buffer space combination was A1B3C1, the indoor air speed increased by 0.1 m/s, and the temperature was 27.0 °C. The optimization results of the two buffer space combinations were between the air speed range of 0.05~0.20 m/s [14] and the thermal comfort of 26~28 °C [38], as shown in Figure 14.

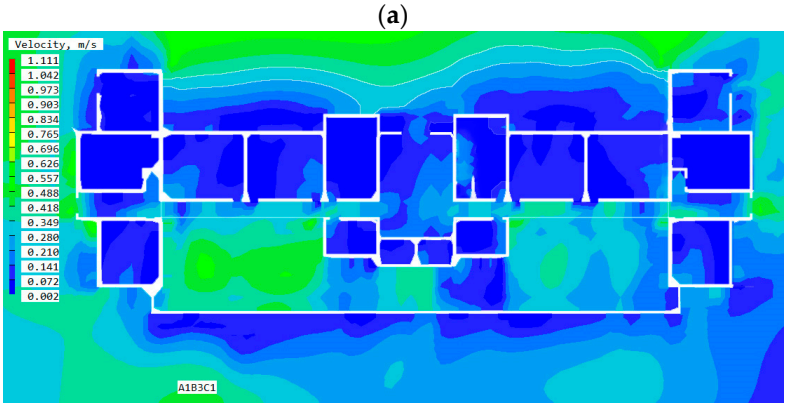
Table 17. Multiple comparisons between different levels of the foyer.

Dependent Variable: Room Temperature LSD		Mean Difference (I − J)			95% Confidence Interval	
(I) Foyer	(J) Foyer		Standard Error	Significance	Lower Limit	Upper Limit
7.2 × 6 × 3.3	7.2 × 8 × 3.6	0.633 *	0.0720	0.013	0.324	0.943
	7.2 × 10 × 3.9	0.433 *	0.0720	0.027	0.124	0.743
7.2 × 8 × 3.6	7.2 × 6 × 3.3	−0.633 *	0.0720	0.013	−0.943	−0.324
	7.2 × 10 × 3.9	−0.200	0.0720	0.109	−1.510	0.110
7.2 × 10 × 3.9	7.2 × 6 × 3.3	−0.433 *	0.0720	0.027	−0.743	−0.124
	7.2 × 8 × 3.6	0.200	0.0720	0.109	−0.110	0.510

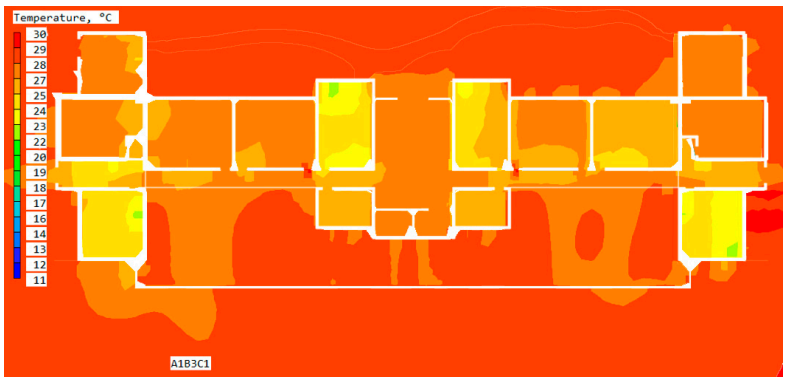
Based on average measured values. The error term is mean square (error) = 0.000. *, The significance level of the mean difference is 0.05.



(**a**)



(**b**)



(**c**)

Figure 14. Perspective view of the optimized air speed and temperature simulation results. (**a**) Refine the rear view perspective; (**b**) air speed simulation results after optimization; (**c**) temperature simulation results after optimization.

Comparing the two optimization schemes A3B2C2 and A1B3C1 with the original building simulation results, it can be found that although the combination A3B2C2 has certain improvement in terms of comfort, it has a large change to the buffer space, such as the corridors and foyer. Compared with A3B2C2, the combination A1B3C1 has fewer changes and is better than the combination A3B2C2 in terms of health, comfort, and economy. Therefore, the combination A1 (16 m × 2 m × 3.3 m), B3 (16 m × 12 m), and C1 (7.2 m × 6 m × 3.3 m) is the optimal combination.

Through the above optimization results, it was found that the buffer space is strongly related to the indoor air speed and thermal environment, and thus, increasing the size of buffer space can promote indoor natural ventilation, reduce indoor temperature, and improve human health and comfort [29,39]. Based on this conclusion, in the renovation design of existing office buildings, the combination of buffer spaces, such as courtyards, corridors, and foyers, can be used to better play the role of the buffer space in improving the indoor air speed and thermal environment, thus meeting people's needs for health and comfort.

5. Discussion

This paper studies the buffer space of case buildings, reveals its relationship with the main interior space, and provides new ideas and methods for the renovation of existing buildings of the same type. The results show that increasing the buffer space size of the building is conducive to improving its thermal buffer effect, promoting indoor natural ventilation, reducing indoor temperature, and improving human health and comfort, indicating the necessity and practical significance of simulating its optimization.

(1) Buffer space optimization is a comprehensive green design and reconstruction strategy. The optimization of buffer space can effectively improve the overall temperature and ventilation effect of building space, so as to improve the environmental quality of buildings.

(2) Thermal regulation of the buffer space. In summer, buffer space can be used for passive buffer precooling of air entering the main interior space, which is conducive to indoor and outdoor thermal exchange [40,41]. At the same time, the ventilation effect brought by different buffer spaces will also play a precooling effect; for example, the corridor buffer space uses the pressure difference brought by the windward side and the leeward side to generate air flow, forming a draft. The longitudinal buffer space can take advantage of the "chimney effect", where hot air rises and fresh air enters from the bottom, carrying out circulating ventilation to carry away excess thermal.

(3) The reasonable layout of buffer space and the good combination of aspect ratio can improve the environment inside the building. Reasonable organization and optimization of the primary and secondary spaces through passive measures can effectively improve the internal environment of the building. According to the connection between different buffer spaces, auxiliary transitional buffer spaces are set up as climate regulation containers, which are used to regulate the microclimate of the main space of the building. This is consistent with the research of Xu X. [42], Shi Feng [43], and Xin Dong [44], who believe that space with a thermal buffer effect can effectively improve the thermal stability and climate adaptability of the interior space of buildings.

However, the content of this study is still limited, and further work needs to be carried out: (1) This paper studies the buffer space of a case building, and the results are applicable to the same type of office buildings, but there is a lack of specific research on different types of buildings. In addition, only summer test data and simulation are available for this case building. In the future, winter data and simulation studies can be added to analyze the thermal buffer potential of buffer space in winter. (2) This paper studies the relationship between building buffer space and interior space, so it excludes the thermal environment factors that cannot be affected by buffer space, including indoor thermal radiation and thermal radiation of the human body and equipment. Dry bulb temperature and air velocity are taken as the main research objects, and future research should consider the

influence of solar radiation on glass and its influence on the average radiant temperature in buildings. (3) The research results and suggestions for the buffer space of the case building are only based on the mesoscopic spatial level of the building, and the detailed structure and building materials of buildings are not taken as the factors studied in this paper. For example, the double-layer skin can also establish a buffer area between buildings and the surrounding environment, and the principle of thermal buffer is also the greenhouse effect and chimney effect. In the following research, we can further study the details of buffer space and buffer space building materials.

6. Conclusions

Based on the thermal buffer effect, this paper studies the buffer space of the case building by Phoenics simulation software, orthogonal test, range and variance qualitative analysis, and draws the following conclusions:

(1) According to the investigation and test results of an office building in Hefei City, the thermal environment of the indoor and outdoor space of the building is poor, which cannot meet the needs of human health and comfort, and it is necessary to adjust the indoor thermal environment by active equipment such as air conditioning. Therefore, the simulation optimization of the case building has certain practical significance.

(2) Through orthogonal experimental simulation, according to the comprehensive analysis of variance and range, when the significance level is $\alpha = 0.05$, when the air speed is used as the evaluation index, the influence of each buffer space on the indoor air speed and thermal environment is ranked as follows: courtyard > corridor > foyer. When the temperature is used as the evaluation index, the influence of each buffer space on the indoor air speed and thermal environment is ranked as follows: courtyard > foyer > corridor.

(3) Through the comprehensive analysis of range and variance, two optimal buffer space combinations were obtained as follows. When the buffer space combination is corridor (16 m × 3 m × 3.9 m), courtyard (16 m × 10 m), and hall (7.2 m × 10 m × 3.6 m), the result of simulation optimization is that the indoor air speed is increased by 0.12 m/s, and the indoor temperature is 27.1 °C. When the buffer space combination is corridor (16 m × 2 m × 3.3 m), courtyard (16 m × 12 m), and hall (7.2 m × 6 m × 3.3 m), the result of simulation optimization is that the indoor air speed is increased by 0.1 m/s, and the indoor temperature is 27.0 °C. The optimization results of the two buffer space combination schemes were in the air speed range of 0.05~0.30 m/s and the thermal comfort of the human body between 26 °C and 28 °C. Compared with the two different combinations, it can be found that the combined corridor (16 m × 2 m × 3.3 m), courtyard (16 m × 12 m), and foyer (7.2 m × 6 m × 3.3 m) have fewer changes to the original building during the renovation, so it is finally selected as the best combination.

Author Contributions: Conceptualization, S.G. and W.C.; methodology, W.C.; software, W.C.; validation, S.G., W.C. and J.F.; formal analysis, W.C. and J.F.; investigation, W.C. and J.F.; resources, S.G.; data curation, S.G. and W.C.; writing—original draft preparation, S.G. and W.C.; writing—review and editing, S.G. All authors have read and agreed to the published version of the manuscript.

Funding: Anhui Provincial Housing and Urban-Rural Construction Science and Technology Program (2022-YF163); Provincial Natural Science Research Key Project of Universities in Anhui Province (KJ2021A0613); Director Fund of Anhui Provincial Key Laboratory of Huipai Architecture (HPJZ-ZRJJ202304); Anhui Provincial Key Laboratory of Green Building and Prefabricated Construction Open Fund Project (No. 2022-JKYL-004); Research Start-up Project of Anhui Jianzhu University (2019QDZ50).

Data Availability Statement: The raw data supporting the conclusions of this article will be made available by the authors upon request.

Conflicts of Interest: The authors declare no conflicts of interest.

References

1. International Energy Agency Buildings Home Page. Available online: https://www.iea.org/energy-system/buildings (accessed on 10 November 2023).
2. *The 14th Five-Year Plan for Building Energy Conservation and Green Building Development*; Ministry of Housing and Urban-Rural Development of the People's Republic of China: Beijing, China, 2022.
3. Sarran, L.; Hviid, A.C.; Rode, C. How to ensure occupant comfort and satisfaction through deep building retrofit? Lessons from a Danish case study. *Sci. Technol. Built Environ.* **2023**, *29*, 2194196. [CrossRef]
4. Simone, P.; Marco, L.; Daniel, A.H. Hygrothermal simulation challenges: Assessing boundary condition choices in retrofitting historic European buildings. Energy Amp; Build. 2023, 297, 113464. [CrossRef]
5. Robert, A.S.; Ilaria, B. Supporting climate-neutral cities with urban energy modeling: A review of building retrofit scenarios, focused on decision-making, energy and environmental performance, and cost. *Sustain. Cities Soc.* **2023**, *98*, 104832. [CrossRef]
6. Sameh, M.; Mutasim, B.; Adel, J. Improving thermal environment for school buildings in Palestine, the role of passive design. *J. Phys. Conf. Ser.* **2019**, *1343*, 012190. [CrossRef]
7. Yu, T.; Zhan, X.; Tian, Z.; Wang, D. A Machine Learning-Based Approach to Evaluate the Spatial Performance of Courtyards—A Case Study of Beijing's Old Town. *Buildings* **2023**, *13*, 1850. [CrossRef]
8. Sun, W.; Chen, L.; Suolang, B.; Liu, K. An Investigation of the Energy-Saving Optimization Design of the Enclosure Structure in High-Altitude Office Buildings. *Buildings* **2024**, *14*, 645. [CrossRef]
9. Li, J. Research on the Passive Regulation Effect of Mediated Space. Ph.D. Thesis, Tsinghua University, Beijing, China, 2017.
10. Weng, W. Research on the Correlation Mechanism and Optimization Strategy between Gray Space Morphology and Thermal Comfort in University Campus. Master's Thesis, Southeast University, Nanjing, China, 2021. [CrossRef]
11. Cheng, H.; Li, P.; Li, X. Regulation strategy of buffer space under high cold climate: A case study of local dwellings in Tibet. *Inter. Des. Decor.* **2023**, *1*, 122–123.
12. Song, Y.H.; Li, D. Overall ecological architecture concept, ecosystem structural framework and bioclimatic buffer layer. *Archit. J.* **1999**, *3*, 4–9+65.
13. Li, G.; Xiang, B. Research on typology of architectural cavity. *Archit. J.* **2006**, *11*, 18–21.
14. Deng, M.; Guo, H.; Xiong, S. Effect and Simulation analysis of building cavity on indoor wind environment. *J. South China Univ. Technol. (Nat. Sci. Ed.)* **2017**, *45*, 74–81. [CrossRef]
15. Wang, X.; Lei, Z.; Chen, J. Modern design transformation of "thick" ecological experience in Zhuangkuo in Hehuang area, Qinghai: A case study of the design of Hehuang Folk Culture Museum. *World Archit.* **2021**, *92–95*, 125. [CrossRef]
16. Chen, X.; Cai, M. Measured and analysis of the thermal buffer effect of building space level: A case study of Nanjing. *Archit. J.* **2022**, 31–34.
17. Zhao, H.; Fu, X.; Zang, Z. Thermal Buffer Effect and Plane Layout Optimization Analysis of Auxiliary Space: A Case Study of a Large Number of Ordinary Office Buildings in Economically Developed Areas. *Archit. Tech.* **2020**, *7*, 86–91.
18. Tong, Y.; Chen, Y. Study on optimization of energy saving design of urban residential buildings in Qinghai—Take Xining as an example. *J. Archit.* **2022**, *S2*, 35–41.
19. *JGJ/T347-2014*; Building Thermal Environment Test Method Standard. Ministry of Housing and Urban-Rural Development of the People's Republic of China. China Architecture & Building Press: Beijing, China, 2014.
20. Duan, Z.; Fang, H.; Li, J. Study on outdoor wind environment measurement and PHOENICS simulation comparative analysis—Take Xuzhou high-rise community as an example. *Art Archit.* **2019**, *9*, 124–126.
21. Wu, Z. Research on indoor wind environment based on CFD numerical simulation. *J. Anhui Eng. Univ.* **2019**, *34*, 85–90.
22. *JGJ/T67-2019*; Design Standard for Office Buildings. Ministry of Housing and Urban-Rural Development of the People's Republic of China. China Architecture and Construction Industry Press: Beijing, China, 2019.
23. *DB34/T5060-2016*; Energy-saving Design Standard of Public Buildings in Hefei City. Anhui Provincial Department of Housing and Urban-Rural Development, China Architecture and Construction Industry Press: Beijing, China, 2017.
24. Zhaosong, F.; Yuchun, Z.; Yanping, Y. Experimental investigation of standard effective temperature (SET*) adapted for human walking in an indoor and transitional thermal environment. *Sci. Total Environ.* **2021**, *793*, 148421. [CrossRef] [PubMed]
25. Devi, S.M.; Ebin, H.; Sheetal, A. Evaluating the Impact of Transition spaces on the Indoor comfort conditions of a Naturally Ventilated Institution Building. *IOP Conf. Ser. Earth Environ. Sci.* **2023**, *1210*, 012014. [CrossRef]
26. Yu, J.; Yifan, Y.; Hang, Y. The impact of thermal environment of transition spaces in elderly-care buildings on thermal adaptation and thermal behavior of the elderly. *Build. Environ.* **2023**, *228*, 109871. [CrossRef]
27. Xiao, B. The regulation effect of building buffer space on indoor and outdoor environmental performance. *Inter. Des. Decor.* **2019**, *10*, 136–137.
28. Yang, F.; Wang, R. An Empirical Study on the Thermal Environment Regulation Efficiency of Climate Buffer Space for High-rise Residential Buildings in Shanghai. *Build. Sci.* **2019**, *35*, 1–10+88. [CrossRef]
29. Xiao, B.; Hong, X. Reference of traditional building buffer space design method based on thermal comfort improvement. *Eco-City Green Build.* **2018**, *4*, 62–67.
30. Anom, P.R.; Atik, P.; Debby, S. Thermal Comfort Of The Outdoor Transition Space In the Dean's Office Building. *IOP Conf. Ser. Earth Environ. Sci.* **2021**, *738*, 012002. [CrossRef]

31. Afreen, S.; Nath, S.S. Computer Simulation Study of Thermal Comfort in Transition Space of an Institutional Building in Jaipur City. *J. Prog. Civ. Eng.* **2020**, *2*, 11.
32. Zhang, Y.; Liu, J.; Zheng, Z. Analysis of thermal comfort during movement in a semi-open transition space. *Energy Build.* **2020**, *225*, 110312. [CrossRef]
33. Chi, M. Research on Natural Ventilation Mode Based on Building Heat Buffer Space Hierarchy. Master's Thesis, Southeast University, Nanjing, China, 2022. [CrossRef]
34. Zhong, H.; Yin, F. *IBM SPSS Statistical Analysis and Application*; China Economic Press: Beijing, China, 2018.
35. Shao, T.; Zheng, W. Energy saving sensitivity analysis of rural residential space design factors based on performance difference of envelope structure. *Build. Sci.* **2021**, *37*, 101–110+125. [CrossRef]
36. Chen, W.; Li, Y.; Cao, D. Research on indoor lighting optimization strategy for renovation of large-span old industrial buildings. *Ind. Constr.* **2022**, *52*, 139–145. [CrossRef]
37. Cao, T. Research on Building Cavity Design Based on Indoor Thermal Environment Improvement. Master's Thesis, Southeast University, Nanjing, China, 2017.
38. *GB50736-2012*; Design Code for Heating, Ventilation and Air Conditioning of Civil Buildings. China Academy of Building Research, China Architecture & Building Press: Beijing, China, 2012.
39. Chen, M. The application of thermal buffering technology in building energy efficiency. *Build. Technol.* **2010**, *41*, 638–640.
40. Li, M.; Guo, J.; Jin, Y. Research on summer thermal performance of buffer space of farm house courtyard based on thermal comfort. *Build. Energy Effic.* 2022; 50, 64–100, (In Chinese and English). [CrossRef]
41. Carlos, J.S. Simulation of the influence of an attic on the building energy efficiency in the Portuguese climate. *Indoor Built Environ.* **2016**, *25*, 674–690. [CrossRef]
42. Xu, X.; Luo, F.; Wang, W.; Hong, T.; Fu, X. Performance-Based Evaluation of Courtyard Design in China's Cold-Winter Hot-Summer Climate Regions. *Sustainability* **2018**, *10*, 3950. [CrossRef]
43. Shi, F.; Jin, W. Research on the design concept and type of building thermal buffer space: A case study of the International Solar Decathlon competition]. *South. Archit.* **2018**, 60–66. [CrossRef]
44. Dong, X.; Yang, Z.; Xu, Y. Climate adaptability study on the roof buffer space of traditional Tujia folk dwellings. *IOP Conf. Ser. Mater. Sci. Eng.* **2019**, 609. [CrossRef]

Disclaimer/Publisher's Note: The statements, opinions and data contained in all publications are solely those of the individual author(s) and contributor(s) and not of MDPI and/or the editor(s). MDPI and/or the editor(s) disclaim responsibility for any injury to people or property resulting from any ideas, methods, instructions or products referred to in the content.